J|A|C|S
ARTICLES
Published on Web 12/03/2002

Direct Electrochemistry of a Bacterial Sulfite Dehydrogenase

Kondo-François Aguey-Zinsou,[†] Paul V. Bernhardt,*[,†] Ulrike Kappler,[‡] and Alastair G. McEwan[‡]

Contribution from the Departments of Chemistry and Microbiology & Parasitology, Centre for Metals in Biology, University of Queensland, Brisbane, 4072, Australia.

Received August 27, 2002; E-mail: P.Bernhardt@mailbox.uq.edu.au.

Abstract: Sulfite dehydrogenase from *Starkeya novella* is an $\alpha\beta$ heterodimer comprising a 40.6 kDa subunit (containing the Mo cofactor) and a smaller 8.8 kDa heme *c* subunit. The enzyme catalyses the oxidation of sulfite to sulfate with the natural electron acceptor being cytochrome c_{550}. Its catalytic mechanism is thought to resemble that found in eukaryotic sulfite oxidases. Using protein film voltammetry and redox potentiometry, we have identified both Mo- and heme-centered redox responses from the enzyme immobilized on a pyrolytic graphite working electrode: $E_{m,8}$ ($Fe^{III/II}$) +177 mV; $E_{m,8}$ ($Mo^{VI/V}$) +211 mV and $E_{m,8}$ ($Mo^{V/IV}$) −118 mV vs NHE; Upon addition of sulfite to the electrochemical cell a steady-state voltammogram is observed and an apparent Michaelis constant (K_m) of 26(1) μM was determined for the enzyme immobilized on the working electrode surface, which is comparable with the value obtained from solution assays.

Introduction

Mononuclear molybdenum enzymes are found in all forms of life.[1−3] In all known cases, the Mo ion at the active site is bound by either one or two molybdopterin ligands (MoCo), each of which acts as a bidentate (dithiolene) chelate for the metal.[4,5] The mononuclear Mo enzymes fall into three distinct groups comprising the xanthine oxidase, sulfite oxidase, and DMSO reductase families (Chart).[6] The ligand "X" in the DMSO reductase family is provided by a serine, cysteine or selenocysteine residue.

Chart 1

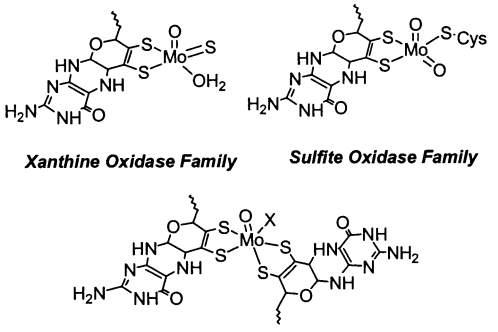

The sulfite oxidase family of molybdoenzymes comprises both plant assimilatory nitrate reductases and sulfite-oxidizing enzymes from eucarya and bacteria, both of which catalyze a direct oxidation of sulfite to sulfate. These sulfite-oxidizing enzymes can be separated into two classes, the sulfite oxidases (SO, mainly found in eucarya) and the sulfite dehydrogenases (SDH), based on their ability to transfer electrons to molecular oxygen, whereas both types can be addressed as sulfite:acceptor oxidoreductases. Most attention has been devoted to SO from eukaryotic organisms, particularly those from human,[7−10] rat,[11] and chicken liver,[12] which catalyze the final step in the degradation of S-containing amino acids such as cysteine or methionine. Chicken and human SO share 68% sequence identity. A crystal structure of chicken liver SO identified a homodimeric protein comprising distinct Mo-binding, dimerization, and heme-binding domains within each momomer.[13] This crystal structure in combination with EPR,[14] ELDOR,[15,16] ESEEM,[17,18] Raman,[19] EXAFS,[20,21] and MCD[22,23] spectroscopic studies has revealed an active site comprising a Mo ion

[†] Department of Chemistry.
[‡] Department of Microbiology and Parasitology.

(1) Rajagopalan, K. V. *Handb. Met.-Ligand Interact. Biol. Fluids: Bioinorg. Med.* **1995**, *1*, 250−256.
(2) Hille, R. *Chem. Rev.* **1996**, *96*, 2757−2816.
(3) Mendel, R. R.; Schwarz, G. *Crit. Rev. Plant Sci.* **1999**, *18*, 33−69.
(4) Kisker, C.; Schindelin, H.; Baas, D.; Retey, J.; Meckenstock, R. U.; Kroneck, P. M. H. *FEMS Microbiol. Rev.* **1998**, *22*, 503−521.
(5) Schindelin, H.; Kisker, C.; Rajagopalan, K. V. *Adv. Protein Chem.* **2001**, *58*, 47−94.
(6) Hille, R. *J. Biol. Inorg. Chem.* **1996**, *1*, 397−404.
(7) Garrett, R. M.; Bellissimo, D. B.; Rajagopalan, K. V. *Biochim. Biophys. Acta* **1995**, *1262*, 147−149.
(8) Garrett, R. M.; Johnson, J. L.; Graf, T. N.; Feigenbaum, A.; Rajagopalan, K. V. *Proc. Natl. Acad. Sci. U.S.A.* **1998**, *95*, 6394−6398.
(9) Temple, C. A.; Graf, T. N.; Rajagopalan, K. V. *Arch. Biochem. Biophys.* **2000**, *383*, 281−287.
(10) Leimkuhler, S.; Rajagopalan, K. V. *J. Biol. Chem.* **2001**, *276*, 1837−1844.
(11) Garrett, R. M.; Rajagopalan, K. V. *J. Biol. Chem.* **1996**, *271*, 7387−7391.
(12) Ratnam, K.; Brody, M. S.; Hille, R. *Prepr. Biochem. Biotechnol.* **1996**, *26*, 143−154.
(13) Kisker, C.; Schindelin, H.; Pacheco, A.; Wehbi, W. A.; Garrett, R. M.; Rajagopalan, K. V.; Enemark, J. H.; Rees, D. C. *Cell* **1997**, *91*, 973−983.
(14) Astashkin, A. V.; Raitsimring, A. M.; Feng, C.; Johnson, J. L.; Rajagopalan, K. V.; Enemark, J. H. *J. Am. Chem. Soc.* **2002**, *124*, 6109−6118.
(15) Enemark, J. H.; Codd, R.; Astashkin, A. V.; Raitsimring, A. M.; Pacheco, A. *Abstr. Pap.−Am. Chem. Soc.* **2000**, *220th*, INOR-008.
(16) Codd, R.; Astashkin, A. V.; Pacheco, A.; Raitsimring, A. M.; Enemark, J. H. *J. Biol. Inorg. Chem.* **2002**, *7*, 338−350.
(17) Raitsimring, A. M.; Pacheco, A.; Enemark, J. H. *J. Am. Chem. Soc.* **1998**, *120*, 11 263−11 278.
(18) Astashkin, A. V.; Mader, M. L.; Pacheco, A.; Enemark, J. H.; Raitsimring, A. M. *J. Am. Chem. Soc.* **2000**, *122*, 5294−5302.

10.1021/ja028293e CCC: $25.00

Scheme 1

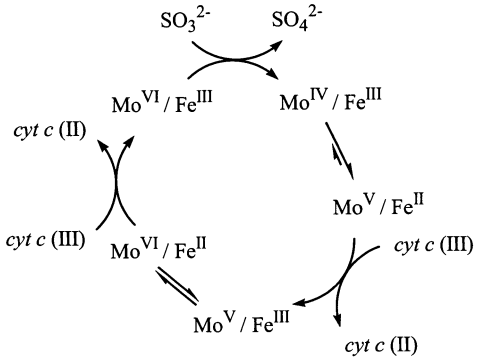

coordinated to a single bidentate pyranopterin-dithiolene chelate, a cysteine residue and two cis oxo ligands. The coordination geometry is square pyramidal, with one of the oxo-groups occupying the apical position.

The catalytic mechanism of SO from chicken liver has been investigated by stopped flow kinetic measurements.[24,25] The overall reaction catalyzed by sulfite oxidase is given in eq 1

$$SO_3^{2-} + 2\ cyt^{III}\ c + H_2O \rightarrow SO_4^{2-} + 2H^+ + 2\ cyt^{II}\ c \quad (1)$$

Computational studies[26] and model systems[27−31] have also contributed to the understanding of structural and mechanistic aspects within the sulfite oxidase family. As illustrated in Scheme 1, the electron-transfer mechanism in this system is quite intricate.

Being a multi-centered enzyme, intramolecular electron transfer between the Mo and heme cofactors of SO is fundamental to the function of the enzyme. It is known that the 2-electron oxidation of SO_3^{2-} occurs upon reaction with the equatorial Mo^{VI}═O moiety. Not shown in Scheme 1 are the ligand exchange reactions that occur, including proton transfer, at each step. These are described in eqs 2a−e. Oxidation of the substrate occurs upon nucleophilic attack by sulfite on the equatorial oxo ligand coupled with an intramolecular two-electron reduction of the Mo ion to generate a $Mo^{IV}-OSO_3$ transient, which undergoes aquation to release sulfate and the tetravalent Mo complex as shown in eq 2a and b. The enzyme is restored to its active form by sequential single-electron oxidations mediated by the heme *b* or *c* cofactor to a *c*-type cytochrome (equations 2c and 2e). Electron equilibration occurs in the intermediate one-electron reoxidized species (equation 2d) and anion and pH dependence of this equilibrium has been investigated with the rates of forward and back electron transfer determined[32,33]

$$Mo^{VI}{=}O{:}Fe^{III} + SO_3^{2-} \rightarrow Mo^{IV}-O-SO_3^{2-}{:}Fe^{III} \quad (2a)$$

$$Mo^{IV}-O-SO_3^{2-}{:}Fe^{III} + H_2O \rightarrow Mo^{V}-OH{:}Fe^{II} + SO_4^{2-} + H^+ \quad (2b)$$

$$Mo^{V}-OH{:}Fe^{II} + cyt^{III}\ c \rightarrow Mo^{V}-OH{:}Fe^{III} + cyt^{II}\ c \quad (2c)$$

$$Mo^{V}-OH{:}Fe^{III} \leftrightarrow Mo^{VI}{=}O{:}Fe^{II} + H^+ \quad (2d)$$

$$Mo^{VI}{=}O{:}Fe^{II} + cyt^{III}\ c \rightarrow Mo^{VI}{=}O{:}Fe^{III} + cyt^{II}\ c \quad (2e)$$

By contrast with eukaryotic systems, examples of sulfite-oxidizing enzymes isolated from bacteria[34,35] and plants[36−38] are much less common. Recently, the isolation and characterization of SDH from *Starkeya novella*[39] was reported. The enzyme, known as the sulfite:acceptor oxidoreductase (SOR) AB protein, exhibits high affinity to both sulfite and the electron acceptor cytochrome *c* and has a catalytic mechanism resembling that of the eukaryotic SOs.[40] In contrast to eukaryotic SOs, SDH is an $\alpha\beta$ heterodimer comprising a 40.6 kDa subunit (containing the Mo cofactor) and a smaller 8.8 kDa heme *c* subunit. The enzyme has an isoelectric point of pH 5.5[40] and is thought to reside in the periplasm of the organism as does its natural electron acceptor, a cytochrome c_{550}. Like the majority of bacterial SDHs, the enzyme is involved in chemolithotrophic sulfur compound oxidation.[35,40,41]

The potential employment of SO in amperometric biosensors has been long recognized.[42,43] Sulfite is an important preservative in foods and beverages and its analytical determination in solution[44−47] and in the gas phase (as SO_2)[48] has been the subject of many investigations. Most of these devices employ artificial electron-transfer mediators (oxidants) such as tetrathiafulvalene tetracyanoquinodimethane,[49] ferricyanide,[50] and *p*-benzoquino-

(19) Garton, S. D.; Garrett, R. M.; Rajagopalan, K. V.; Johnson, M. K. *J. Am. Chem. Soc.* **1997**, *119*, 2590−2591.
(20) George, G. N.; Garrett, R. M.; Graf, T.; Prince, R. C.; Rajagopalan, K. V. *J. Am. Chem. Soc.* **1998**, *120*, 4522−4523.
(21) George, G. N.; Pickering, I. J.; Kisker, C. *Inorg. Chem.* **1999**, *38*, 2539−2540.
(22) Helton, M. E.; Pacheco, A.; McMaster, J.; Enemark, J. H.; Kirk, M. L. *J. Inorg. Biochem.* **2000**, *80*, 227−233.
(23) McNaughton, R. L.; Tipton, A. A.; Rubie, N. D.; Conry, R. R.; Kirk, M. L. *Inorg. Chem.* **2000**, *39*, 5697−5706.
(24) Hille, R. *J. Biol. Inorg. Chem.* **1997**, *2*, 804−809.
(25) Brody, M. S.; Hille, R. *Biochemistry* **1999**, *38*, 6668−6677.
(26) Thapper, A.; Deeth, R. J.; Nordlander, E. *Inorg. Chem.* **1999**, *38*, 1015−1018.
(27) Izumi, Y.; Glaser, T.; Rose, K.; McMaster, J.; Basu, P.; Enemark, J. H.; Hedman, B.; Hodgson, K. O.; Solomon, E. I. *J. Am. Chem. Soc.* **1999**, *121*, 10 035−10 046.
(28) Mader, M. L.; Carducci, M. D.; Enemark, J. H. *Inorg. Chem.* **2000**, *39*, 525−531.
(29) Thapper, A.; Lorber, C.; Fryxelius, J.; Behrens, A.; Nordlander, E. *J. Inorg. Biochem.* **2000**, *79*, 67−74.
(30) Lim, B. S.; Willer, M. W.; Miao, M.; Holm, R. H. *J. Am. Chem. Soc.* **2001**, *123*, 8343−8349.
(31) Nagarajan, K.; Chaudhury, P. K.; Srinivasan, B. R.; Sarkar, S. *Chem. Commun.* **2001**, 1786−1787.
(32) Sullivan, E. P., Jr.; Hazzard, J. T.; Tollin, G.; Enemark, J. H. *Biochemistry* **1993**, *32*, 12 465−12 470.
(33) Pacheco, A.; Hazzard, J. T.; Tollin, G.; Enemark, J. H. *J. Biol. Inorg. Chem.* **1999**, *4*, 390−401.
(34) Wodara, C.; Bardischewsky, F.; Friedrich, C. G. *J. Bacteriol.* **1997**, *179*, 5014−5023.
(35) Kappler, U.; Dahl, C. *FEMS Microbiol. Lett.* **2001**, *203*, 1−9.
(36) Jolivet, P.; Bergeron, E.; Meunier, J.-C. *Phytochemistry* **1995**, *40*, 667−672.
(37) Ganai, B. A.; Masood, A.; Baig, M. A. *Phytochemistry* **1997**, *45*, 879−880.
(38) Eilers, T.; Schwarz, G.; Brinkmann, H.; Witt, C.; Richter, T.; Nieder, J.; Koch, B.; Hille, R.; Hansch, R.; Mendel, R. R. *J. Biol. Chem.* **2001**, *276*, 46 989−46 994.
(39) Kelly, D. P.; McDonald, I. R.; Wood, A. P. *Int. J. Syst. and Evol. Microbiology* **2000**, *50*, 1792−1802.
(40) Kappler, U.; Bennett, B.; Rethmeier, J.; Schwarz, G.; Deutzmann, R.; McEwan, A. G.; Dahl, C. *J. Biol. Chem.* **2000**, *275*, 13 202−13 212.
(41) Kelly, D. P.; Shergill, J. K.; Lu, W. P.; Wood, A. P. *Ant. Van Leeuwenhoek Int. J. Gen. Mol. Microbiol. Immunol.* **1997**, *71*, 95−107.
(42) Matsumoto, K.; Matsubara, H.; Ukeda, H.; Osajima, Y. *Agric. Biol. Chem.* **1989**, *53*, 2347−2353.
(43) Mulchandani, A.; Groom, C. A.; Luong, J. H. T. *J. Biotechnol.* **1991**, *18*, 93−102.
(44) Campanella, L.; Cipriani, P.; Martini, T. M.; Sammartino, M. P.; Tomassetti, M. *Anal. Chim. Acta* **1995**, *305*, 32−41.
(45) Pabel, B. *Lebensmittelchemie* **1999**, *53*, 61.
(46) Situmorang, M.; Hibbert, D. B.; Gooding, J. J.; Barnett, D. *Analyst* **1999**, *124*, 1775−1779.
(47) Abass, A. K.; Hart, J. P.; Cowell, D. *Sensors and Actuators, B: Chemical* **2000**, *B62*, 148−153.
(48) Hart, J. P.; Abass, A. K.; Cowell, D. *Biosensors & Bioelectronics* **2002**, *17*, 389−394.

ne[51] that shuttle electrons away from the active site following sulfite oxidation. Furthermore, these so-called enzyme electrodes typically employ an indirect determination of sulfite through the amperometric determination of H_2O_2 produced (in reaction with coadsorbed peroxidase)[52] or O_2 consumed[53] during sulfite oxidation. Immobilization of SO onto the electrode surface is a prerequisite and a number of polymer matrixes have been employed including polypyrrole,[54] chitosan-poly(hydroxyethyl methacrylate)[51] and polytyramine.[46]

Despite the intense interest in the electrochemical properties of SO both in biology and analytical chemistry, it is perhaps ironic that a direct voltammetric response from the (Mo) active site has never been observed. Instead, the use of artificial mediators, both in potentiometry and in voltammetry, has been necessary to observe indirect electrocatalytic activity from eukaryotic SOs in a few isolated cases, including microcoulometry[55] and cyclic voltammetry[56−58] of chicken liver SO.

Herein, we report the first direct electrochemistry of SDH from *S. novella*. We have identified Mo and Fe-based voltammetric responses from the enzyme in the absence of substrate. Furthermore, we show that catalytic activity is retained upon immobilization of the enzyme on an edge oriented pyrolytic graphite working electrode.

Experimental Section

Materials. SorAB (SDH) from *S. novella* was prepared as previously described.[40] All other reagents were obtained commercially.

Electrochemical Measurements. Voltammetry was performed with a BAS100B/W electrochemical workstation employing an edge-plane pyrolytic graphite working electrode, an Ag/AgCl reference electrode and Pt counter electrode. All measurements were performed at 25 °C inside a Belle Technologies Glovebox at an O_2 concentration of less than 2 ppm.

Electrode Preparation. A clean working electrode surface (0.09 cm^2) was obtained by cleaving a ca. 1 μm layer from the face of the electrode with a microtome followed by sonication in MilliQ water. No abrasives were used. Two methods of electrode modification were then explored that both gave reproducible and stable voltammetric responses. The first comprised coadsorption of the enzyme within a didodecyldimethylammonium bromide (DDAB) surfactant film as described previously.[59,60] Briefly, the surfactant film was prepared by mixing of 5 μL of enzyme (100 μM) and 5 μL of DDAB (2 mM) then coating the electrode surface with 2 μL of this mixture before allowing the film to dry overnight at 6 °C. The second method involved coating the clean working electrode surface with 5 μL of polylysine solution (1 g/mL) then allowing the solution to dry at room temperature for 2 h. Thereafter, 3 μL of the enzyme (100 μM) was deposited on the polylysine modified electrode and again air-dried. In each case, the electrochemical cell contained ca. 500 μL of solution with 0.01 M NaBr as supporting electrolyte. For experiments conducted at the pH optimum (pH 8.0) the electrolyte contained 50 mM Tris buffer, while for varying pH experiments a buffer mixture of bis-tris propane (10 mM) and 2-amino-2-methylpropan-1-ol (10 mM) titrated with the appropriate amount of acetic acid was employed to give a final pH in the range 5 to 10.

Redox Potentiometry. Heme redox potentials were determined by standard redox potentiometric methods with all measurements performed within a glovebox under an atmosphere of N_2 (concentration of O_2 < 2 ppm).[61] The mediators used were phenazine methosulfate (1 μM) and 2-hydroxy-1,4-naphthaquinone (5 μM), the reductant was $Na_2S_2O_4$ and the oxidant was $K_3[Fe(CN)_6]$. The solution pH was adjusted with acetic acid before each titration and the solution potential was measured upon equilibration with an ABB Kent Taylor combination Pt−Ag/AgCl electrode attached to a Hanna 8417 meter. Spectral differences between the oxidized and reduced heme were monitored at 416 nm with a Shimadzu UV Mini 1240 spectrophotometer. The midpoint potentials at each pH (E_m) were calculated from eq 3; a combination of the Beer−Lambert and Nernst equations for a single electron redox couple (*ox* + e^- *red*) involving two absorbing species at 25 °C.

$$A = \left[\frac{\epsilon_{ox}10^{\frac{E-E_m}{59}} + \epsilon_{red}}{10^{\frac{E-E_m}{59}} + 1}\right] C_{enz} \qquad (3)$$

In this case, A is the absorbance of the solution at 416 nm, ϵ_{ox} and ϵ_{red} are the extinction coefficients of the ferric and ferrous heme chromophores at the same wavelength, C_{enz} is the total enzyme concentration and E is the observed potential. Reversibility of each reductive titration was established by back-titration with $[Fe(CN)_6]^{3-}$. All potentials are cited versus the Normal Hydrogen Electrode.

Kinetic Analysis. The variation of the observed limiting catalytic current (i_{lim}) as a function of substrate concentration (C_{sub}) followed Michaelis−Menten kinetics[62] and the data were fit to eq 4

$$i_{lim} = \frac{i_{max}C_{sub}}{C_{sub} + K_m} \qquad (4)$$

where i_{max} is the saturation limiting current and K_m is the apparent Michaelis constant.

The pH profile for catalytic activity was fit to a model where the intermediate (singly protonated) form is the catalytically competent species. The data followed eq 5 where the catalytic current is equated to enzyme activity[25]

$$i_{lim} = \frac{i_{opt}}{1 + 10^{(pk_{a1}-pH)} + 10^{(pH-pk_{a2})}} \qquad (5)$$

In this case pK_{a1} and pK_{a2} are the lower and higher protonation constants respectively and i_{opt} is the limiting current at the optimal pH value.

Results and Discussion

The benefits and advances in protein voltammetry, particularly under turnover conditions, have been well documented.[63] The ability to monitor the catalytic performance of an enzyme film as a function of both electrochemical potential and time in the absence of complications due to mediators or protein diffusion provides insight into electron and atom transfer mechanisms,

(49) Korell, U.; Lennox, R. B. *J. Electroanal. Chem.* **1993**, *351*, 137−143.
(50) Svitel, J.; Stredansky, M.; Pizzariello, A.; Miertus, S. *Electroanalysis* **1998**, *10*, 591−596.
(51) Ng, L.-T.; Yuan, Y. J.; Zhao, H. *Electroanalysis* **1998**, *10*, 1119−1124.
(52) Menzel, C.; Lerch, T.; Scheper, T.; Schuegerl, K. *Anal. Chim. Acta* **1995**, *317*, 259−264.
(53) Xie, X.; Shakhsher, Z.; Suleiman, A. A.; Guilbault, G. G.; Yang, Z.; Sun, Z.-a. *Talanta* **1994**, *41*, 317−321.
(54) Adeloju, S. B.; Shaw, S. J.; Wallace, G. G. *Electroanalysis* **1994**, *6*, 865−870.
(55) Spence, J. T.; Kipke, C. A.; Enemark, J. H.; Sunde, R. A. *Inorg. Chem.* **1991**, *30*, 3011−3015.
(56) Coury, L. A., Jr.; Oliver, B. N.; Egekeze, J. O.; Sosnoff, C. S.; Brumfield, J. C.; Buck, R. P.; Murray, R. W. *Anal. Chem.* **1990**, *62*, 452−458.
(57) Coury, L. A., Jr.; Murray, R. W.; Johnson, J. L.; Rajagopalan, K. V. *J. Phys. Chem.* **1991**, *95*, 6034−6040.
(58) Coury, L. A., Jr.; Yang, L.; Murray, R. W. *Anal. Chem.* **1993**, *65*, 242−246.
(59) Zhang, Z.; Nassar, A.-E.; Lu, Z.; Schenkman, J. B.; Rusling, J. F. *J. Chem. Soc., Faraday Trans.* **1997**, *93*, 1769−1774.
(60) Aguey-Zinsou, K.-F.; Bernhardt, P. V.; McEwan, A. G.; Ridge, J. P. *J. Biol. Inorg. Chem.* **2002**, *7*, 879−883.
(61) Dutton, P. L. *Methods Enzymol.* **1978**, *54*, 411−435.
(62) Anderson, L. J.; Richardson, D. J.; Butt, J. N. *Faraday Discussions* **2000**, *116*, 155−169.
(63) Armstrong, F. A.; Wilson, G. S. *Electrochim. Acta* **2000**, *45*, 2623−2645.

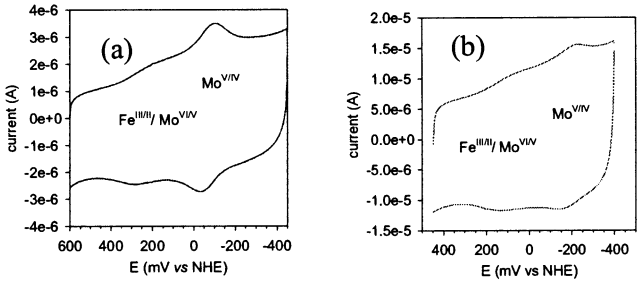

Figure 1. (a) Cyclic voltammogram of SDH at DDAB surfactant film-modified edge-plane pyrolytic graphite working electrode (scan rate 100mV s^{-1}, pH 8.0); (b) cyclic voltammogram of SDH at polylysine-modified working electrode (scan rate 100 mV s^{-1}, pH 8.0).

particularly in multi-centered enzymes. Direct voltammetric investigations of Mo enzymes in general are rare and those extant have appeared very recently. These reports have involved the enzymes nitrate reductase[62,64,65] and DMSO reductase (from *Rhodobacter capsulatus* and *E. coli*).[60,66] Although catalytic voltammetry of nitrate reductase[62,64,65] and *E. coli* DMSO reductase[66] was demonstrated, no voltammetric response from the Mo active site of these enzymes was observed in the absence of substrate.

Nonturnover Cyclic Voltammetry. A recent paper from this group[60] reported the first example of a Mo-based response from an enzyme in the absence of substrate with DMSO reductase from *R. capsulatus*, where distinct $Mo^{VI/V}$ and $Mo^{V/IV}$ couples were seen. In this work, we have identified nonturnover voltammetric responses from the heme ($Fe^{III/II}$) and Mo ($Mo^{VI/V}$ and $Mo^{V/IV}$) centers of SDH adsorbed to a pyrolytic graphite electrode. The cyclic voltammogram of SDH is shown in Figure 1a where the surface of the pyrolytic graphite electrode was modified by a DDAB surfactant film. A broad higher potential response is seen in addition to a more pronounced lower potential wave. Square wave voltammetry enabled the resolution of the higher potential wave into two one-electron responses in the lower pH region. The voltammetric responses are symmetrical and their current maxima each increase linearly with scan rate, which is evidence for reversible, surface-confined electron transfer. An enzyme surface population of 4.1×10^{-12} mol (or 4.5×10^{-11} mol cm^{-2}) was calculated from the scan rate dependence of the current maxima. This is about the degree of coverage expected for a monolayer of protein ($\sim 2 \times 10^{-11}$ mol cm^{-2} for a spherical protein of diameter 50 Å and density of about 1 g cm^{-3}).

The pH dependence of the Mo-based couples determined by square wave voltammetry are presented in Figure 2 and the data appear in Table 1. The higher potential $Mo^{VI/V}$ couple exhibits a shift of −59 mV/pH unit, which is consistent with the uptake of a single proton upon one-electron reduction. The potential of the $Mo^{V/IV}$ couple is pH independent in the range $5 < pH < 10$, although the current response is attenuated at the low pH end of this range. The heme $Fe^{III/II}$ couple is only resolved in the voltammetry experiments below pH 7.

Similar voltammetric responses were obtained using a polylysine-coated working electrode (Figure 1b). In this case, a

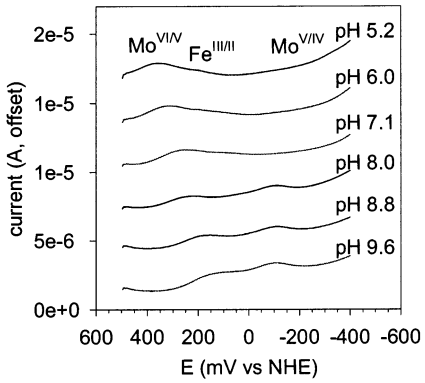

Figure 2. pH-Dependent square wave voltammograms of SDH (potential step 4 mV, square wave amplitude 15 mV, square wave frequency 5 mV).

Table 1. pH Dependence of Redox Potentials (mV vs NHE) Determined Voltammetrically and Potentiometrically (n.r. not resolved; n.d not determined)

	DDAB surfactant film (voltammetry)			potentiometry
pH	$Mo^{VI/V}$	$Mo^{V/IV}$	$Fe^{III/II}$	$Fe^{III/II}$
5.2	+381	−113	+203	n.d.
6.0	+319	−120	+195	n.d
7.1	+264	−113	n.r.	+189
8.0	+211	−118	n.r.	+177
8.8	+164	−118	n.r.	+168
9.6	+104	−120	n.r	+153

Scheme 2

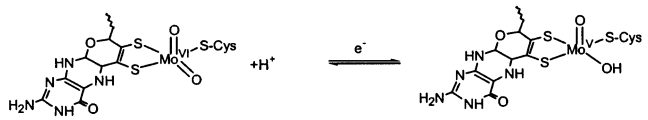

3-fold greater electrode coverage was obtained (1.7×10^{-10} mol cm^{-2}). In addition to the apparently greater enzyme coverage, catalytic activity (see below) was far superior on this electrode surface compared with the DDAB-modified electrode. The apparent Mo and Fe-centered redox potentials were ca. 100 mV more negative than those determined on the DDAB-modified electrode, although the separation of the couples was the same regardless. The origin of the cathodic shift in the observed potentials is uncertain. The pH dependence of the voltammetry on the polylysine modified electrode was the same as that found for the DDAB modified electrodes (data not shown).

In each case, the pH dependence of the higher potential Mo response is consistent with Scheme 2, and with ESEEM spectroscopy on chicken liver SO[18] where an exchangeable (OH) proton was identified close to the active site of the pentavalent Mo ion.

The heme $Fe^{III/II}$ midpoint potential was determined by redox potentiometry using the differential electronic absorption spectra of the ferric and ferrous forms as the measure of Fe reduction. Optical absorption by the Mo chromophore is negligible in this region and so the $Fe^{III/II}$ potential could be determined without interference from the Mo centers in contrast to that seen in the cyclic voltammograms (Figure 1a and 1b). The heme redox potential was determined at four pH values (Table 1). The modest pH dependence ($\sim$10 mV/pH unit) mirrors microcoulometric and potentiometric results with eukaryotic sulfite oxidases,[55] and indicates no proton transfer reactions are occurring close to the active site of the heme cofactor upon

(64) Anderson, L. J.; Richardson, D. J.; Butt, J. N. *Biochemistry* **2001**, *40*, 11 294−11 307.
(65) Butt, J. N.; Anderson, L. J.; Rubio, L. M.; Richardson, D. J.; Flores, E.; Herrero, A. *Bioelectrochemistry* **2002**, *56*, 17−18.
(66) Heffron, K.; Leger, C.; Rothery, R. A.; Weiner, J. H.; Armstrong, F. A. *Biochemistry* **2001**, *40*, 3117−3126.

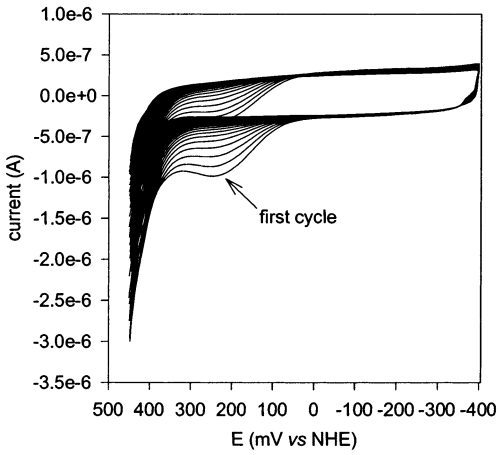

Figure 3. Steady state cyclic voltammograms of SDH in the presence of 300 μM SO_3^{2-}. The catalytic current decreases with increasing number of scans.

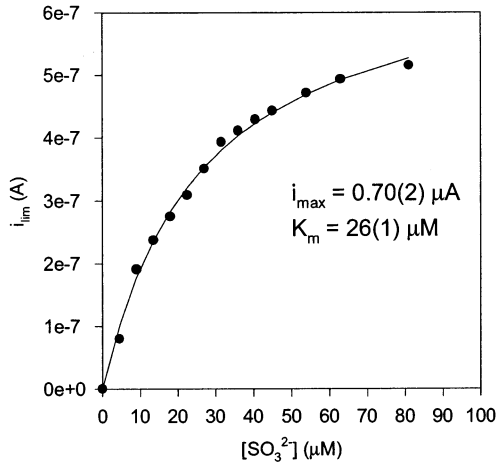

Figure 4. Plot of the steady state voltammetric current (i_{lim}) as a function of SO_3^{2-} concentration.

reduction. The axially bound ligands in the heme *c* cofactor of*S. novella* SDH are not known, but in the heme *b* cofactor of chicken liver SO they are histidine residues as shown by crystallography.[13]

Catalytic Voltammetry. Introduction of sulfite to the electrochemical cell resulted in a pronounced change in the voltammetric response from transient (peak) to steady state (sigmoidal) coupled with an amplification of the observed current (Figure 3). Repeated cycling led to a marked diminution of the catalytic current. It is known that most SO/SDH enzymes undergo product inhibition in assay studies, and in this case it appears that a similar effect is being observed.

Saturation of the catalytic current (taken from the first cycle) occurred at ca. 40 μM sulfite and an apparent Michaelis constant (K_m) of 26(1) μM was determined (Figure 4). This value is consistent with that obtained from a solution steady-state enzyme assay (27 μM).[40] For comparison, the K_m value of 16 μM for chicken liver SO has been reported.[25]

The pH dependence of the saturation catalytic current (from the first cyclic voltammogram) is shown in Figure 5. The profile is distinctly bell-shaped, showing a maximum at about pH 8.5. From the pH profile, we have determined two pK_a values for an active site where the intermediate (monoprotonated) species

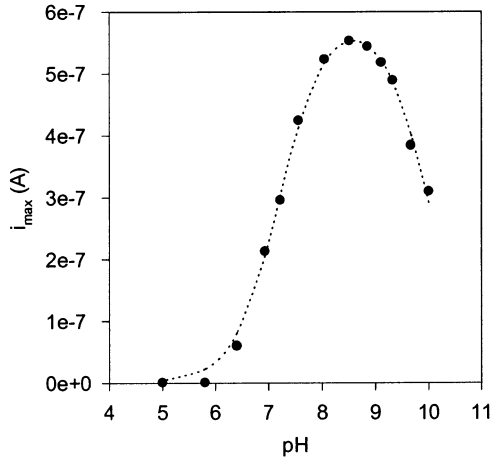

Figure 5. pH-Dependence of catalytic current maximum for SO_3^{2-} oxidation by SDH.

is the active form. From this analysis, pK_a values of 7.2 and 10.0 were determined.

In all known SOs, there is a tyrosine residue close to the active site that is believed to be responsible for stabilizing the bound substrate through a hydrogen bonding PhOH···O−S−O−Mo interaction during catalysis. On this basis, the higher pK_a value may be assigned to deprotonation of this tyrosine residue leaving the phenolate residue incapable of stabilizing the coordinated oxoanion. A similar pK_a value of 9.3 was found for chicken liver SO and was assigned to the corresponding conserved Y322 residue.[25] The origin of the lower pK_a value is uncertain. The substrate pK_a (HSO_3^-/SO_3^{2-}) is 7.2, and this is possibly related to the loss of turnover activity. However, a kinetic analysis of chicken liver SO found that both sulfite and bisulfite were oxidized at similar rates. Below pH 7, the $Mo^{VI/V}$ potential becomes significantly more positive than the heme couple and this may also inhibit the rate of electron egress from the Mo active site, presumably more efficiently achieved via the heme cofactor. Alternatively, it is possible that key surface amino acids on either the heme-binding or Mo-containing subunit become protonated at this point and electron flow between the two subunits is switched off. In the absence of a crystal structure, we cannot offer any other explanation for the lower pH limb of the catalytic profile.

Although SDH from *S. novella* exhibits a number of properties characteristic of eukaryotic SOs such as inhibition by anions such as phosphate, sulfate and nitrate, there are some significant differences that point to active site diversity in the bacterial enzyme.[40] First, it does not exhibit the characteristic low-pH EPR spectrum of chicken liver sulfite oxidase, nor does it exhibit the so-called phosphate inhibited EPR signal (although phosphate is an inhibitor of SDH), which has been suggested to reflect inflexibility at the active site of the bacterial enzyme. Second, *S. novella* SDH is an $\alpha\beta$-heterodimer, in contrast to homodimeric eukaryotic SOs with each monomer comprising Mo- and heme-binding domains covalently linked by a flexible 10 amino acid loop. The actual disposition of the two subunits in chicken liver SO has been a subject of considerable interest. In the crystal structure conformation of chicken liver SO, the Mo and Fe atoms are about 32 Å apart. Notwithstanding,electron transfer between these two centers in solution has been found[32,33] to be much faster ($\sim 10^3$ s^{-1}) than one would expect on the basis of theoretical predictions[67] for this internuclear separation.

An explanation for this phenomenon[33] is that the protein adopts an entirely different conformation during electron transfer from Mo to Fe whereby the heme binding domain swings around to be in proximity to the Mo cofactor. More recently, ELDOR spectroscopy has been used to support this hypothesis,[16] and a broad distribution of conformations was found. The dynamics of this conformational change were also found to be dependent on the solvent viscosity.[68]

There is no covalent link between the Mo-binding and heme-binding subunits in *S. novella* SDH and we plan to investigate some of these features soon. Finally, the heme *c* cofactor in *S. novella* SDH is in contrast to the *b*-type hemes found in all eukaryotic SOs. We are currently pursuing a crystal structure of this enzyme, which will hopefully aid in the interpretation of some of these observations.

(67) Gray, H. B.; Winkler, J. R. *Annu. Rev. Biochem.* **1996**, *65*, 537−561.
(68) Feng, C.; Kedia, R. V.; Hazzard, J. T.; Hurley, J. K.; Tollin, G.; Enemark, J. H. *Biochemistry* **2002**, *41*, 5816−5821.

Conclusions

We have demonstrated that catalytic activity of SDH from *S. novella* may be realized while the enzyme is immobilized to the surface of an electrochemical working electrode. We have shown that electron exchange between the working electrode and the redox active subunits is facile and that similar kinetic behavior as found in solution assays can be maintained in this system without the need for artificial electron-transfer mediators.

Acknowledgment. Financial assistance from the Australian Research Council and the University of Queensland is gratefully acknowledged.

Note added in Proof: Enemark, Armstrong, and co-workers have recently reported the direct electrochemistry of chicken liver sulfite oxidase, where a non-turnover response from the heme subunit was seen, but not from the Mo cofactor (*J. Am. Chem. Soc.* **2002**, *124*, 11 612−11 613).

JA028293E